

# Turbidity under changing physical forcing over two contrasting locations of seagrass meadows



João D. Lencart e Silva†, Ana Azevedo†, Ana Isabel Lillebø‡, João Miguel Dias†

†CESAM & Physics Dept., University of Aveiro, 3810-193 Aveiro, Portugal  
j.lencart@ua.pt  
de.azevedo@ua.pt  
joao.dias@ua.pt

‡CESAM & Dept. of Biology, University of Aveiro, 3810-193 Aveiro, Portugal  
lillebo@ua.pt

[www.cerf-jcr.org](http://www.cerf-jcr.org)



## ABSTRACT

Lencart e Silva, J. D., Azevedo, A., Lillebø, A.I., Dias, J.M., 2013. Turbidity and seagrass meadows under changing physical forcing. In: Conley, D.C., Masselink, G., Russell, P.E. and O'Hare, T.J. (eds.), *Proceedings 12<sup>th</sup> International Coastal Symposium* (Plymouth, England), *Journal of Coastal Research*, Special Issue No. 65, pp. 2023-2028, ISSN 0749-0208.

[www.JCRonline.org](http://www.JCRonline.org)

Seagrass meadows support a range of ecosystem functions in coastal lagoons, from habitat and shelter of invertebrates and fishes to stabilizing sediments, serving at the same time as important ecological quality status indicators due to their sensitivity to water quality parameters. Seagrass meadows are recognized as one of the most productive ecosystems on Earth. Those in mesotidal mid-latitude lagoons with low flushing times primary production are greatly affected by turbidity. Here, we investigate the physical controls of turbidity in Ria de Aveiro, Portugal, by simulating its response to varying conditions of tidal and river forcing. A 2-dimensional hydrodynamic and transport model developed and calibrated for this coastal lagoon was forced with tide at the inlet, wind and river inflow. The tidal flow was found to be the main driver of changes in turbidity with river-borne plumes assuming some relevance during extreme events. The turbidity response for scenarios of increasing storm-driven events and mean sea level was compared between two existent seagrass patches and the differences in the turbidity conditions put in context of their relevant physical mechanisms. A difference in response was shown to exist between the two patches, mainly attributable to the tide which resuspends the spatially-varying sediments deposited seasonally by river inflow.

**ADDITIONAL INDEX WORDS:** *hydrodynamic modelling, cohesive sediments, mesotidal forcing, Ria de Aveiro, coastal lagoon.*

## INTRODUCTION

Coastal lagoons are recognised as highly productive environments, providing valuable natural resources for the vicinity human populations. These coastal systems are unique ecosystems, to which the increasing pressures in coastal zones, from both natural and anthropogenic factors, make them particularly sensitive to physical change. Mesotidal coastal lagoons with relevant freshwater input show a strong influence of physical forcing in the distribution and characteristics of the biotic component of these ecosystems. Shifts in the intensity, timing and mechanism of the physical forcing can lead to important changes in the biological characteristics of a lagoon.

Seagrasses are flowering plants that generally grow in soft substrates of marine and estuarine systems, providing a wide variability of ecosystem services (Barbier *et al.*, 2011). In the Ria de Aveiro lagoon, seagrass meadows were formerly abundant in both subtidal and intertidal environments, with relevant contributions for the lagoon's productivity. These important habitats have been under a considerable decline, following the worldwide trend. In Azevedo *et al.* (2013) a DPSIR (Drivers-Pressures-State-Impacts-Response) analysis is made on the current state of the Ria de Aveiro seagrass meadows. Silva *et al.* (2004) attributed changes in seagrass communities of Ria de Aveiro lagoon to the increased resuspension and turbidity in the water column, as a result of the artificial dredging by harbour

authorities. This has consequences in the propagation of the tide inside the lagoon, leading to increased velocities in the dredged channels.

The Ria de Aveiro (Figure 1a) consists of four main channels which radiate from the mouth with several branches, islands and mudflats. The lagoon is mesotidal with an average tidal range of 2 m (tidal amplitude at the inlet ranges from 0.6 m in neap tides to 3.2 m in spring tides) (Dias *et al.*, 2000). Due to the combined effects of the freshwater discharge and tidal propagation, the central area of the Ria de Aveiro exhibits a longitudinal salinity gradient from ~0 in the upper reaches of the Espinheiro channel to ~36 at the bar entrance (Vaz and Dias, 2008). The tidal flow dominates the transport for the better part of the hydrological cycle. However, due to the seasonality of the rainfall and the fast response of part of the catchment draining into the lagoon, after strong rainfall events the rivers can increase their flow in 2 orders of magnitude and the lagoon is flooded with freshwater. Under these conditions estuarine circulation assumes a greater influence in the transport of dissolved and suspended substances, mainly at the head of the channels (Vaz *et al.*, 2012). The average depth of the lagoon relative to chart datum is about 1 m, except in the navigation channels where dredging operations are frequently carried out. Due to the shallow depth and to the tidal wave amplitude the intertidal area is a significant part of the total area being studied.

Here we make a sensitivity analysis to the impact of changes in physical forcing in the lagoon's turbidity by using the concentration of Total Suspended Solids (TSS) as a proxy for turbidity. Resorting to hydrodynamic and sediment transport

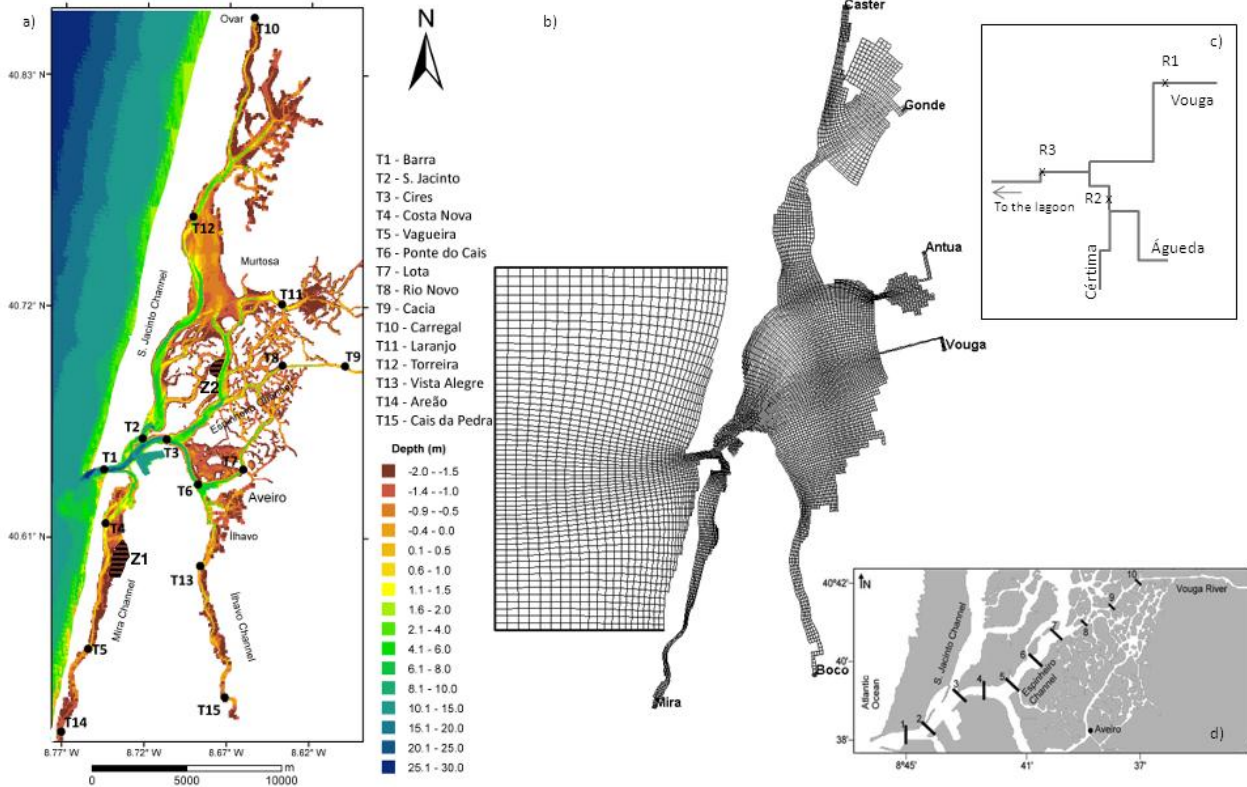


Figure 1. (a) Study area, bathymetry and stations used in the calibration of the tide, shaded areas indicating *Zostera* patches used in the analyses; (b) numerical grid, discharge locations and open boundary (thick line); (c) schematic diagram of the location of the hydrometric stations (d) stations used in the calibration of heat and salt according to Vaz and Dias (2008).

Table 1. Erosion  $\tau_{ce}$  and deposition  $\tau_{cd}$  critical shear stress for sediment calibration runs.

$\tau_{ce}$	$\tau_{cd}$ ( $Nm^{-2}$ )	$\tau_{ce}$		
		0.30	0.45	0.60
0.075	A	D	G	
0.150	B	E	H	
0.300	C	F	I	

numerical modelling we calculate the *TSS* concentration for a set of scenarios of *TSS* discharge by the rivers into the lagoon. The changes in mean sea level in the context of climate change can trigger significant changes in the way the tide propagates inside the lagoon by decreasing depth-averaged drag and thus lead to an increase in amplitude in both free surface elevation and velocity. In turn, these changes may induce changes in the spatial distribution of sediments at the bed and in the resuspension regime. The changes caused by this mechanism are akin to those caused by the increase in velocity due to dredging. Given that deepening the channels is proposed as one of the causes for seagrass losses, deeper water due to a rise in mean sea level is tested here as one of the possible future changes in physical controls to turbidity.

To gauge the combined effect of changes in the river runoff regime and sea-level rise we analyse the *TSS* concentration at two different sites (Z1 and Z2, Figure 1) of know *Zostera noltii* meadows. These sites are both placed in the intertidal. However, site Z1 is less exposed to the effect of the Vouga, the main river

discharging into the lagoon, closer to the inlet and in a channel which approximates a classical conical shaped estuary. The site Z2 is situated in a zone where the velocity field is affected by the complex bathymetry.

## METHODS

### Numerical Model

Delft3D-Flow is a three-dimensional, finite differences hydrodynamic and transport model which simulates flow and transport resulting from tidal and meteorological forcing. In the present application, the hydrodynamic model solves the Navier-Stokes shallow water equations with hydrostatic, Boussinesq and f-plane approximations (WL|DelftHydraulics, 1996; Lesser *et al.*, 2004). Delft3D-Flow uses a horizontal Arakawa-C grid with control volumes and for most applications an Alternating Direction Implicit (ADI) integration method. The Delft3D-Flow platform has been used previously in estuarine conditions under mesotidal forcing in, e.g. Tomales Bay California (Harcourt-Baldwin and Diedericks, 2006).

A Cartesian, curvilinear orthogonal grid was designed to represent the main hydrodynamic features of the lagoon with the minimum number of calculation points. An offshore zone was set to allow for the dissipation of spurious open boundary effects before reaching the mouth of the lagoon. This grid has 267x164 cells calculating the solution at 9828 points. An open boundary at the shelf was defined for the segments represented in Figure 1b. The curvilinear properties of the grid allow a ~30 m resolution in

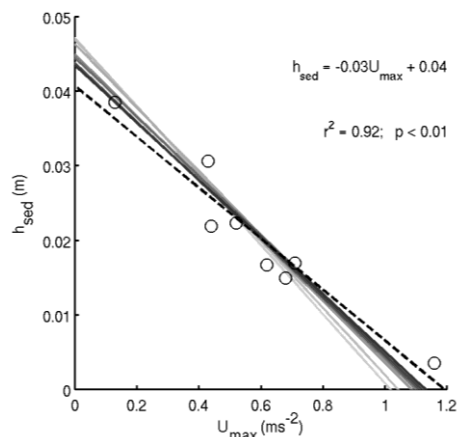


Figure 2. Relation between local velocity maxima and local cohesive sediment thickness at the bed. Circles and dashed line: results and regression model from Rodrigues *et al.* 2011; gray lines from light to dark: runs A to I of Table 1.

narrow tidal channels and a  $\sim 700$  m resolution at the offshore open boundary. A 2-dimensional depth-averaged approximation was made given that the Ria de Aveiro is mostly a vertically well-mixed system (Vaz and Dias, 2008). The bathymetry of the Ria de Aveiro used here results from the interpolation to the numerical grid of a set of topo-hydrographic surveys from 1987-88, 2003 and 2011. The interpolation was a piecewise, exclusive process starting with the most recent survey and moving to earlier surveys where later data was unable to provide a solution (Figure 1a).

The propagation of the tide was modelled by prescribing the main 19 astronomic constituents determined at the mouth of the Ria de Aveiro, with phase and amplitude corrected for the open boundary and calibrating its propagation through the adjustment of the bottom roughness. This parameter assumes the Manning formulation of the Chezy coefficient (WL|DelftHydraulics, 1996). To represent accurately the propagation of the tide in the lagoon, the model simulates wet and drying of the intertidal areas for a water level threshold of 0.1 m. To reproduce wind driven circulation, a spatially-constant wind momentum flux prescribed.

The heat model uses air temperature, the combined net (short wave) solar and net (long wave) atmospheric radiation, relative humidity and wind speed to calculate heat losses due to evaporation, back radiation and convection. Boundary conditions for temperature are prescribed at the oceanic open boundary and a total of 6 freshwater points were defined as outflows representing the Vouga, Antuã, Boco, Caster, Gonde and the system of streams discharging at head of the Mira Channel. The transport of salt is calculated taking into account the input of freshwater from the catchment and the salinity prescribed at the oceanic open boundary. Precipitation and evaporation are not taken into account in the mass balance.

Delft3D-Flow allows the simulation of sediment suspended-load transport dynamics using the 3-dimensional advection-diffusion equation (WL|DelftHydraulics, 1996). In this application, transport is computed for the 2-dimensional domain used in the hydrodynamic solution. The characterization of the sediment properties in the model is made by prescribing density of sediment, settling velocity, vertical diffusion coefficient for erosion and critical shear stresses for settling and erosion. In this application, sediment thickness at the bottom is updated whilst not

changing the bathymetry used in the calculation of hydrodynamic quantities. A single fraction of cohesive sediment was modelled, representing sediment with a grain size  $< 63 \mu\text{m}$ , not taking into account the effect of salinity in flocculation of sediments nor changes in fluid density due to suspended-load concentration. The transport, erosion and settling of cohesive sediment is simulated by prescribing a space-varying initial bed thickness and by taking into account the input of suspended-load from the catchment.

### Calibration of the Hydrodynamics

The 19 harmonic constituents imposed at the boundary were modified in phase, to taking into account the distance between the open boundary and the tide gauge location. These harmonic constituents were calculated using a 366 day record where water level was sampled each 6 min between 31/12/2002 and 31/12/2003 (Vaz *et al.*, 2005). The amplitude of the harmonic constituents was adjusted to reflect the depth at the boundary.

A set of runs with the duration of 90 days was performed forcing only the tide at the boundary and comparing model predictions against 15 tide gauge stations (Figure 1a) where time series of SSE were available for at least 30 days length, measured from 2002 to 2004 (Araújo, 2005). The calibration of the bottom roughness through the Manning ( $n$ ) coefficient was performed using the truncated function of depth vs.  $n$  (Picado *et al.*, 2010).

A set of 32 stations along 10 sections of the Espinheiro Channel (Figure 1d) were used to compare the water temperature and salinity model predictions to the observations carried out by Vaz and Dias (2008). In their work, the Espinheiro Channel was sampled fortnightly from September 2003 to September 2004 from the inlet to the mouth of the Vouga, the main river discharging into the lagoon. This transect crosses the lagoon, spanning most of its conditions and receiving the outflow of all of the other channels, thus making a good proxy for the temperature and salinity conditions inside the lagoon.

For the hydrologic year of 2003-2004, time series of wind speed, air temperature and relative humidity from a local weather station (Figure 1a) and radiation from the NCEP reanalysis (Kalnay *et al.*, 1996) were prescribed for the atmospheric boundary. At the open ocean boundary and following Vaz *et al.* (2005) a constant value of temperature ( $15^\circ\text{C}$ ) and salinity (36) was set originally. Improvements in the calibration were sought forcing at the oceanic open boundary a time series for salinity and temperature vertical profile from the HYCOM model (Cummings, 2005). The E-HYPE (Donnelly *et al.*, 2010) freshwater discharge predictions for the Vouga, Antuã and Boco rivers were used as forcing at the respective discharge points. For the Caster, Gonde and Mira system the Boco discharged was assumed.

### Choosing the Cohesive Sediment Parameters

The results of an extensive survey of the benthic communities by Rodrigues *et al.* (2011) show a relation between maximum velocity and the fraction of fines in the erodible bottom sediment (Figure 2). This relation was used to build the initial distribution of fines based on our model's prediction of velocity maximum for each of the calculation points. For that, an erodible 0.05 m layer was assumed and cohesive sediment thickness calculated based on the fraction predicted by the relation in Figure 2.

To test the characteristics of the sediment, the erosion and deposition critical shear stresses were varied according to Table 1, assuming a moderate sedimentation speed of  $0.5 \times 10^{-3} \text{ms}^{-1}$ . The results of the final distribution after a 15-day run with no sediment input were plotted against the velocity maximum for each point of the domain and the regression lines compared with the linear model used to generate the initial condition.

**Initial Condition and Scenarios**

After a 5 day tidal spin-up, a winter spin-up run with ocean and atmospheric forcing was calculated between 01/01/2003 and 30/07/2003. Flow from the E-HYPE model (Donnelly *et al.*, 2010) and solid load from the power law in (1) were prescribed at the discharge locations.

To test the sensitivity of suspended solids to changes in tidal input, a set of scenarios of river input and mean sea level were run between 30/07/2003 and 30/08/2003 (Table 2). Mean sea level rise was set to +0.35 m according to the A1B scenario calculations for the Portuguese coast (Lopes *et al.* 2011). To reflect a possible future increase in extreme events, a frequent 1-year maximum and an extreme 15-year maximum were chosen for solid load input.

**RESULTS**

**River Input: Water and Sediment Loads**

Due to the lack of uniformly available river flow data for the main rivers discharging in the Ria de Aveiro the open access results of the E-HYPE model data were used for the Vouga, Antuã and Boco catchments. To test the validity of the E-HYPE water quantity calculation, the stations R1 and R2 (Figure 1c) were used. Station R1 is placed in the Vouga main catchment and station R2 is placed at the lower reaches of the Cértima, the main tributary before the Vouga discharges into the lagoon. These stations are ~30 km apart with no major tributaries between them but the sum of their flow will not account for the total flow at the mouth of the Vouga. The fitness of the E-HYPE model is compared against the sum of the flows at stations R1 and R2 between 01/02/2002 and 10/01/2008 for a total of 1960 days. The model’s Root Mean Square Error (RMSE) and skill (Warner *et al.*, 2005) were  $54 \text{ m}^3 \text{ s}^{-1}$  and 0.84, respectively.

The flow calculated by E-HYPE for the Vouga and the TSS measurements at R3 were used to establish a relation between fluid ( $Q$ ) and solid load ( $Q_s$ ) through a power law. According to Lane *et al.* (1997), rather than a relation between flow and TSS concentration, there should be a relation between flow and sediment flux and linear regression can be sought between the measured TSS transported by flow modelled by E-HYPE and flow itself:

$$Q_s = Q_m TSS_{SLL} \quad Q_s = \alpha Q_m^\beta \quad (1)$$

where  $Q_m$  is the flow from the E-HYPE model, the TSS measured at R3 and  $\alpha$  and  $\beta$  parameters estimated by least-square-fit, yielding  $\alpha = 9.327$  and  $\beta = 1.063$  for an  $r^2$  of 0.79 and a  $p < 0.001$ .

**Calibration**

The bathymetry was corrected locally where the interpolation method misrepresented finer scale surveys. After these corrections, the use of the best bottom roughness from a set of runs led to a general improvement in the fit. The model has an excellent to very good fit (skill > 0.95 and RMSE < 0.2 m) on most stations, with less impressive performance on isolated inner meandering regions. Figure 3a shows the comparison between model predictions and observations for the main diurnal, semi-diurnal and shallow water harmonic constituents. The model has an excellent agreement on most stations when representing semi-diurnal tide (85% of the variance), a good agreement on most stations when representing diurnal tide (7% of the variance) and a poor agreement representing the quarter-diurnal tide (5% of the variance).

The first results using a constant ocean boundary for water temperature and salinity were encouraging, with salinity and

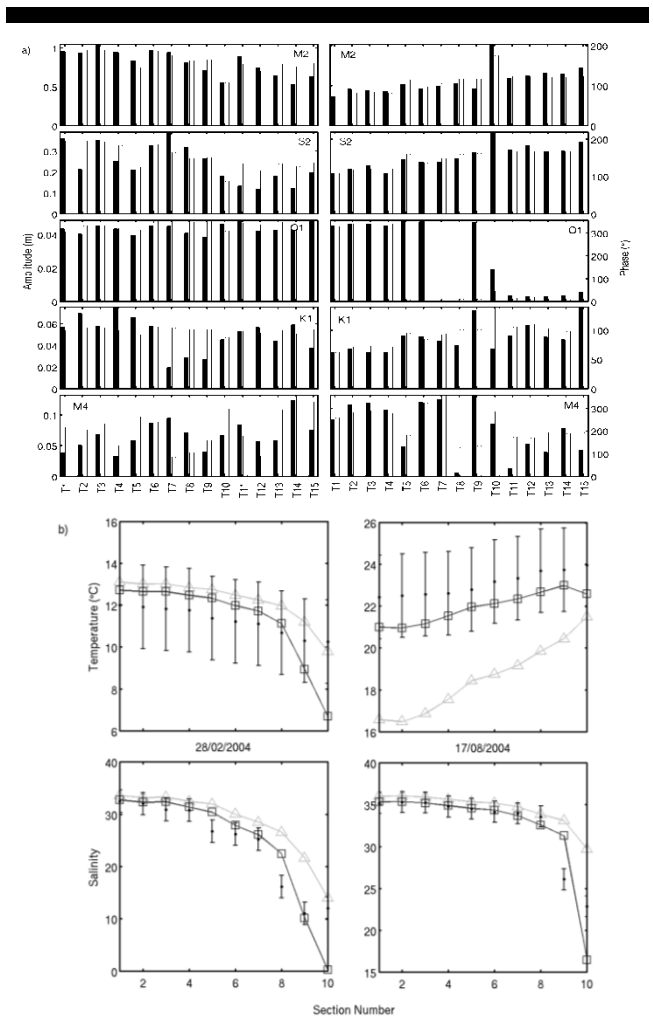


Figure 3. Hydrodynamic model calibration results: (a) harmonic comparison for the 15 tidal stations (black – observed, white – modelled); (b) subset of the 26 surveys analyzed for the Espinheiro Channel representing temperature and salinity surveys in winter and summer (observed -points and error bars, first configuration - gray line, best configuration – black line).

temperature following the observed annual cycle. However, when compared point to point there were significant departures from the observation. Figure 3b shows that for temperature the main problem was the invariable ocean boundary condition, with significant improvement after the addition of the HYCOM series. As for salinity, the boundary condition led to small improvements but the inability to reproduce the low salinities at the upper reaches was only improved when a no-flow-through condition was imposed on the channel walls in the upper reaches of Espinheiro Channel. The model reproduces well the seasonal cycle with an average skill of 0.98 for temperature and 0.86 for salinity. The seasonal-averaged RMSE, bias and Mean Absolute Error (MAE)

Table 2. Run-off return periods ( $T_r$ ) and mean sea level for production runs.

	$T_r$	Dry	1 year	15 years
<b>MSL</b>				
<b>Current</b>		PS1	PS2	PS3
<b>Current + 0.35 m</b>		PS4	PS5	PS6

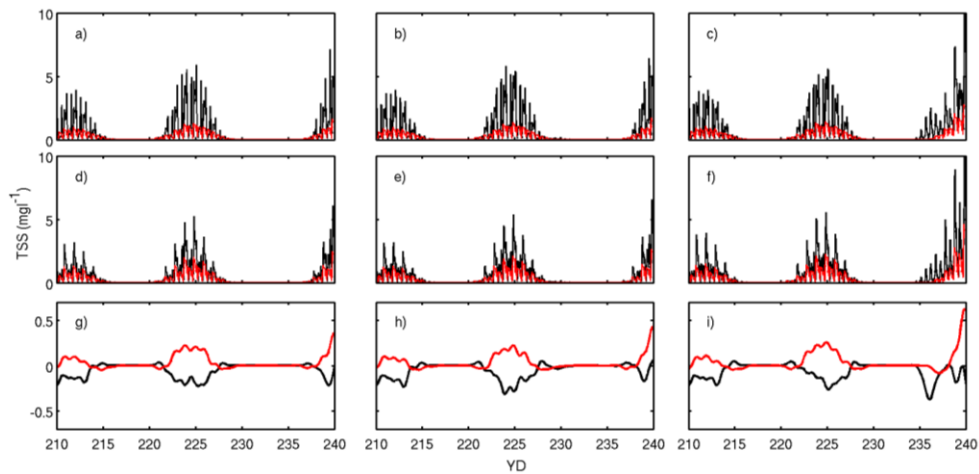


Figure 4. Results for *TSS* concentration (station Z1 - red; station Z2-black). (a) to (c), Current mean sea level scenarios for dry conditions, 1-year maximum and 15-year maximum respectively. (d) to (f) A1B (+0.35m) mean sea level scenarios for dry conditions, 1-year maximum and 15-year maximum respectively. (g) to (i) Differences of *TSS* concentration between current and A1B scenario for dry conditions, 1-year maximum and 15-year maximum respectively.

were 1.1 °C, 0.1 °C and 0.9 °C for temperature, respectively. For salinity these values were 4, 0.1 and 3. In terms of survey to survey spatial fitness of the temperature and salinity gradients, the model under performed for temperature (skill = 0.55) and showed poor results for salinity (skill = 0.75).

Figure 2 shows the results from the testing of critical shear stresses for erosion and deposition detailed in Table 1. In comparison to the Rodrigues *et al.* (2011) surveys used as reference (Figure 2, dashed line), all of the sediment configurations show higher build up of fines at the bed for low velocities and lower build up for high velocities. The closest fit is for the maximum of both critical shear stresses (Table 1, scenario I), representing the sediment with least mobility.

## Scenarios

A 29-year long series of  $Q_s$  was predicted for the 6 discharge locations using the flow from E-HYPE and the 30-day aggregated flow discharging into the bay was calculated for every day in the series:

$$Q_{s_{agg}}(d) = \sum_{i=0}^w Q_s(d-i) \quad (2)$$

where the window size  $w = 30$  days,  $d$  is the day in the series and  $s$  the station index. Yearly maximums for aggregated flow were calculated and a good fit found for the Generalized Extreme Values distribution (GEV) with  $\kappa=-0.11$ ,  $\sigma=51787$  and  $\mu=100839$ . Using the GEV distribution, 1-year and 15-year maximum aggregated solid discharge were calculated and a date was identified for each of these maxima. Flow and solid load were extracted for the 6 discharge locations for the 30-day interval ending on these dates. The resulting flow and solid load series intervals were grafted to the last day of the longest interval of dry conditions in 2003 (30/07/2003). Hence, these scenarios represent the first runoff event after the dry season.

Figure 4 shows the results for *TSS* concentration, spatially-average over each of the two seagrass patches for the scenarios detailed in Table 2. There is a consistent semidiurnal and fortnightly response associated with the variation of tidal energy input at both patches. However, there is a clear difference between

the patches with the station more exposed to the Vouga runoff (Z2) showing higher maxima and wider range in *TSS* concentration. The forcing of runoff events with 1-year and 15-year return periods have little impact in the model results with *TSS* concentration increasing slightly with runoff and more expressively for the Z2 patch. Changes in the mean sea level result in a  $\pm 10\%$  difference in *TSS* in relation to the results at the reference mean sea level.

## DISCUSSION AND CONCLUSIONS

The results for the calibration of the tide show that the model has a very good to excellent fit on most places of the lagoon. Similar results were found with more detailed calculation grids using the ELCIRC finite elements model (Picado *et al.*, 2010). Exceptions to this are the results for the stations closer to the head of the channels. This can be attributed to i) the resolution of the numerical grid in these regions; ii) quality of the observation data there with shorter time series and less than perfect sampling (Araújo, 2005). The poor agreement of the quarter-diurnal (5% of the variance) is connected to the unknown profile of the intertidal flats due to the absence of detailed up-to-date topographic surveys there.

The model showed a good seasonal agreement in the representation of salinity and water temperature along the most representative channel in the lagoon. For temperature, the most significant adjustment to improve fitness was the addition of the HYCOM profile at the ocean open boundary. For salinity the main improvement was the correction of topographic misrepresentations at the upper reaches of the channel. The poorer spatial agreement was mainly due to difficulties in representing sections 8 – 10 (Figure 1d). This is an expected result due to the uncertainty of the E-HYPE daily outputs. This uncertainty is felt to a greater extent nearer the river mouths whilst farther downstream tidal dispersion acts as a low-pass filter in the time domain.

The results for the *TSS* show the increase in concentration from neap to spring tide reported in Martins *et al.* (2009) but our results show an underestimation of concentration reported by those authors. Without a consistent sampling of the *TSS* inside the

lagoon after river runoff events it is difficult to gauge the plausibility of the model's weak response to large increases in river runoff. Several processes missing in the approximations made may account for the model's behaviour. At the beginning of the wet winter season and in the initial stages of a runoff event river data shows higher concentration of solids. The assumption of a nearly constant TSS concentration in the river made in (1) does not take into account this change in concentration and so the input of turbidity plumes may be significantly underestimated. To overcome this difficulty, explicit modelling of solid load at the catchment is needed.

The overestimation of sediment thickness at low velocity sites and the underestimation of the opposite indicate that the sediment type used here is overly mobile (Figure 2). Given that the tested critical shear stresses are in accordance with the particle sizes reported in Martins *et al.* (2009) extra processes may be missing from the formulation. Thus, future work should take into account the three sediment fractions in order to best represent their cumulative effects in reducing the resuspension leading to larger sediment thickness at the bed. Higher residence times of fines in the lagoon could be achieved by making velocity settling dependent of salinity-related flocculation.

This first approach to the modelling of TSS in Ria de Aveiro with realistic tidal and density driven flows and estimated river forcing shows that there is still a great deal to improve in the representation of this process. However, a clear difference of conditions was shown to exist between the two patches of *Zostera noltii* analysed here and these preliminary results isolate the response to tidal forcing as the main physical mechanism causing the changes of turbidity inside the lagoon. The role played by river runoff in turbidity is reflected in the differences of conditions between the two patches, less through direct plume influence but rather through the spatially-varying seasonal deposition of sediments that are then resuspended by the tide. At its current stage of development the model does not confirm the link between changes in physical forcing and an increase in turbidity pointed as a cause for *Zostera noltii* decline in the lagoon. The inclusion of the above mentioned extra processes in the formulation may lead to a shift in weight of the three physical agents analysed here.

### ACKNOWLEDGEMENT

The European Commission, under the 7th Framework Programme, supported this study through the collaborative research project LAGOONS (contract n°283157). The Portuguese Foundation for Science and Technology (FCT) also supported this study through the research projects DyEPlume (PTDC/MAR/107939/2008) and LTER-RAVE (LTER/BIA-BEC/0063/2009) co-funded through European Union (COMPETE, QREN, FEDER) and national FCT/MCES (PIDDAC), as well through the PhD grant SFRH/BD/84613/2012 (A. Azevedo).

### LITERATURE CITED

- Araújo, I.G.B., 2005. Sea level variability: examples from the Atlantic coast of Europe. Ph.D. Thesis, University of Southampton, UK, 216 pp.
- Azevedo, A., Sousa, A.I., Lencart e Silva, J.D., Dias, J.M. and Lillebø, A.I., 2013. Application of the generic DPSIR framework to seagrass communities of Ria de Aveiro: a better understanding of this coastal lagoon In: Conley, D.C., Masselink, G., Russell, P.E. and O'Hare, T.J. (eds.), Proceedings 12th International Coastal Symposium (Plymouth, England), *Journal of Coastal Research*, Special Issue No. 65, pp.
- Barbier, E.B., Hacker, S.D., Kennedy, C., Koch, E.W., Stier, A.C. and Silliman, B.R., 2011. The value of estuarine and coastal ecosystem services. *Ecological Monographs*, 81, 169-193.
- Cummings, J.A., 2005. Operational multivariate ocean data assimilation. *Quarterly Journal of the Royal Meteorological Society*, Part C, 131(613), 3583-3604.
- Dias, J.M.; Lopes, J.F., Dekeyser, I., 2000. Tidal propagation in Ria de Aveiro Lagoon, Portugal. *Physics and Chemistry of the Earth(B)* 25 (4), 369-374
- Donnelly, C., Dahne, J., Rosberg, J., Strömqvist, J., Yang, W. and Arheimer, B., 2010. High-resolution, large-scale hydrological modelling tools for Europe. IAHS Publ. 340:553-561.
- Harcourt-Baldwin, J.L. and Diedericks, G.P.J., 2006. Numerical modelling and analysis of temperature controlled density currents in Tomales Bay, California. *Estuarine, Coastal and Shelf Science*, 66: 417-428.
- Kalnay, E., Kanamitsu, M., Kistler, R., Collins, W., Deaven, D., Gandin, L., Iredell, M., Saha, S., White, G., Woollen, J., Zhu, Y., Leetmaa, A., Reynolds, B., Chelliah, M., Ebisuzaki, W., Higgins, W., Janowiak, J., Mo, K.C., Ropelewski, C., Wang, J., Jenne, R. and Joseph, D., 1996. The NCEP/NCAR 40-Year Reanalysis Project. *Bulletin of the American Meteorological Society*, 77, 437-472.
- Lane, L. J., Hernandez, M., & Nichols, M., 1997. Processes controlling sediment yield from watersheds as functions of spatial scale. *Environmental Modelling & Software*, 12(4), 355-369. doi:10.1016/S1364-8152(97)00027-3.
- Lesser, G.R., Roelvink, J.A., van Kester, J. and Stelling, G.S., 2004. Development and validation of a three-dimensional morphological model. *Coastal Engineering*, 51: 883-915.
- Lopes C.L., Silva P.A., Dias J.M., Rocha A., Picado A., Plecha S. and Fortunato A.B., 2011. Local sea level change scenarios for the end of the 21st century and potential physical impacts in the lower Ria de Aveiro (Portugal). *Continental Shelf Research*, 31, 14, 1515-1526.
- Martins, V., Jesus, C.C., Abrantes, I., Dias, J.M. and Rocha F., 2009. Suspended Particulate Matter vs. Bottom Sediments in a Mesotidal Lagoon (Ria de Aveiro, Portugal). *Journal of Coastal Research*, S156, 1370-1374.
- Picado, A., Dias, J.M. and Fortunato, A., 2010. Tidal changes in estuarine systems induced by local geomorphologic modifications. *Continental Shelf Research*, 30, 17, 1854-1864.
- Rodrigues, A.M., Quintino, V., Sampaio, L., Freitas, R. and Neves R., 2011. Benthic Biodiversity Patterns in Ria de Aveiro, Western Portugal: Environmental-Biological Relationships. *Estuarine Coastal and Shelf Science*, 95, 338-348.
- Silva, J.F., Duck, R.W. and Catarino, J.B., 2004. Seagrasses and sediment response to changing physical forcing in a coastal lagoon. *Hydrology and Earth System Sciences*, 8, 151-159.
- Vaz, N. and Dias, J.M., 2008. Hydrographic Characterization of an Estuarine Tidal Channel. *Journal of Marine Systems*, 70, 168-181.
- Vaz, N., Dias, J.M., Leitão, P. and Martins, I., 2005. Horizontal patterns of water temperature and salinity in an estuarine tidal channel: Ria de Aveiro. *Ocean Dynamics*, 55, 416-429.
- Vaz, N., Lencart e Silva, J.D. and Dias J.M., 2012. Salt fluxes in a complex river mouth system of Portugal. *PLoS ONE*, 7(10): e47349.
- Warner, J. C., Geyer, W. R. and Lerczak, J. A., 2005. Numerical modelling of an estuary: a comprehensive skill assessment. *Journal of Geophysical Research*, 110, C05001.
- WL|DelftHydraulics, 1996. Delft3D-FLOW user manual version 3.05. Delft: WL Hydraulics.